

ARTICLE

DOI: 10.1038/s41467-018-07603-1

OPEN

Human preprocalcitonin self-antigen generates TAP-dependent and -independent epitopes triggering optimised T-cell responses toward immune-escaped tumours

Aurélie Durgeau^{1,2}, Yasemin Virk¹, Gwendoline Gros¹, Elodie Voilin¹, Stéphanie Cognac¹, Fayçal Djenidi¹, Jérôme Salmon³, Julien Adam⁴, Vincent de Montpréville^{1,5}, Pierre Validire⁶, Soldano Ferrone⁷, Salem Chouaib^{1,15}, Alexander Eggermont⁸, Jean-Charles Soria⁹, François Lemonnier¹⁰, Eric Tartour¹¹, Nathalie Chaput^{12,13}, Benjamin Besse¹⁴ & Fathia Mami-Chouaib¹

Tumours often evade CD8 T-cell immunity by downregulating TAP. T-cell epitopes associated with impaired peptide processing are immunogenic non-mutated neoantigens that emerge during tumour immune evasion. The preprocalcitonin (ppCT)₁₆₋₂₅ neoepitope belongs to this category of antigens. Here we show that most human lung tumours display altered expression of TAP and frequently express ppCT self-antigen. We also show that ppCT includes HLA-A2-restricted epitopes that are processed by TAP-independent and -dependent pathways. Processing occurs in either the endoplasmic reticulum, by signal peptidase and signal peptide peptidase, or in the cytosol after release of a signal peptide precursor or retrotranslocation of a procalcitonin substrate by endoplasmic-reticulum-associated degradation. Remarkably, ppCT peptide-based immunotherapy induces efficient T-cell responses toward antigen processing and presenting machinery-impaired tumours transplanted into HLA-A*0201-transgenic mice and in NOD-*scid-Il2r^{null}* mice adoptively transferred with human PBMC. Thus, ppCT-specific T lymphocytes are promising effectors for treatment of tumours that have escaped immune recognition.

¹INSERM UMR 1186, Integrative Tumour Immunology and Genetic Oncology, Gustave Roussy, EPHE, PSL, Fac. de Médecine, Univ. Paris-Sud, Université Paris-Saclay, 94805 Villejuif, France. ²ElyssaMed, Paris Biotech Santé, 75014 Paris, France. ³CNRS (Centre National de la Recherche Scientifique) UMR 8122, Gustave Roussy, Faculté de Médecine, Univ. Paris-Sud, Université Paris-Saclay, 94805 Villejuif, France. ⁴INSERM U 981, Gustave Roussy, Faculté de Médecine, Univ. Paris-Sud, Université Paris-Saclay, 94805 Villejuif, France. ⁵Service d'Anatomie Pathologique, Centre Chirurgical Marie-Lannelongue, 92350 Le-Plessis-Robinson, France. ⁶Service d'Anatomie Pathologique, Institut Mutualiste Montsouris, 75014 Paris, France. ⁷Department of Surgery, Massachusetts General Hospital, Harvard Medical School, Boston, MA 02114, USA. ⁸Cancer Institute, Gustave Roussy Cancer Campus, Grand Paris, 94805 Villejuif, France. ⁹Department of Drug Development (DITEP), Gustave Roussy, 94805 Villejuif, France. ¹⁰Département Endocrinologie, Métabolisme et Diabète, Equipe Immunologie des Diabètes, INSERM U1016, 75014 Paris, France. ¹¹INSERM U970, Paris Cardiovascular Research Centre, Université Paris-Descartes, Sorbonne Paris Cité, Equipe Labellisée Ligue Contre le Cancer, Hôpital Européen Georges Pompidou, Service d'Immunologie Biologique, 75015 Paris, France. ¹²Laboratory of Immunomonitoring in Oncology, and CNRS-UMS 3655 and INSERM-US23, Gustave Roussy Cancer Campus, Villejuif, France. ¹³Faculté de Pharmacie, University Paris-Sud, F-92296 Chatenay-Malabry, France. ¹⁴Département de Médecine, Gustave Roussy, 94805 Villejuif, France. ¹⁵Present address: Thumbay Institute for Precision Medicine, Gulf Medical University, Ajman 4184, UAE. These authors contributed equally: Yasemin Virk, Gwendoline Gros. Correspondence and requests for materials should be addressed to F.M.-C. (email: Fathia.Mami-Chouaib@gustaveroussy.fr)

Cytotoxic T lymphocytes (CTLs) are the major effectors of the immune system capable of eliminating transformed cells following recognition, by the T cell receptor (TCR), of specific antigenic peptides presented by the major histocompatibility complex class I (MHC-I)-beta-2-microglobulin (β 2m) complex. Therefore, immunotherapy strategies have been developed to induce a strong persistent antitumour CTL response in order to destroy primary cancer cells and metastases. Current immunotherapies consist of stimulating tumour-specific T cells via therapeutic vaccination of cancer patients with tumour-associated antigens (TAA) or adoptively transferring in vitro expanded native or engineered T lymphocytes targeting malignant cells^{1,2}. Moreover, identification of T cell surface molecules such as CTL-associated antigen-4 (CTLA-4) and programmed death-1 (PD-1), involved in regulation of antigen-specific T cell responses, has recently led to the development of promising new immunotherapies against cancer^{3–6}. Indeed, treatment of cancer patients with neutralizing monoclonal antibodies (mAbs) specific to these T cell inhibitory receptors has resulted in impressive response rates and, in some cases, durable remission, emphasizing the central role of endogenous T lymphocytes in defence against malignant cells. In this context, it has been reported that tumour regression following therapeutic PD-1 blockade requires pre-existing CD8⁺ T lymphocytes that are negatively regulated by PD-1/PD-ligand 1 (PD-L1)-mediated adaptive immune resistance⁷. More recent studies demonstrated that T cell reactivity towards tumour-specific mutated antigens, called neoantigens, is directly associated with clinical benefits of adoptive T cell therapy, immune checkpoint blockade and peptide-based cancer vaccines^{8–17}. This implies that, in responding patients, endogenous T lymphocytes are able to recognize peptide neoepitopes displayed on the surface of malignant cells by MHC molecules and to trigger antitumour immune responses.

Unfortunately, only a fraction of cancer patients respond to these T cell-based therapeutic interventions, indicating that multiple additional mechanisms leading to tumour resistance to immunotherapy exist. In this context, it was recently demonstrated that patients identified as non-responders to anti-CTLA-4 mAbs have tumours with genomic defects in interferon (IFN)- γ pathway genes¹⁸. Moreover, primary or acquired resistance to PD-1 blockade immunotherapy was associated with defects in pathways involved in IFN- γ -receptor signalling and antigen presentation by MHC-I molecules^{19,20}. Among additional known mechanisms involved in tumour resistance to T cell-mediated immunity, alterations in antigen processing play an important role. Indeed, accumulating evidence indicates that defects in transporter associated with antigen processing (TAP) subunits result in a sharp decrease in surface expression of MHC-I/peptide complexes, enabling escape of malignant cells from CD8 T cell recognition. In this regard, it was recently reported that T lymphocytes specific to a non-mutated self-epitope derived from the C-terminus region of the TRH4 protein, defined as a T cell epitope associated with impaired peptide processing (TEIPP), were efficiently selected in the thymus of TCR transgenic mice and might be activated by peptide-based vaccination, leading to growth control of TAP-deficient tumours expressing low levels of MHC-I/peptide complexes²¹. In humans, we had previously identified a non-mutated tumour epitope derived from the pre-procalcitonin (ppCT) signal peptide (ppCT_{16–25}) by a mechanism independent of proteasomes and TAP, involving signal peptidase (SP) and signal peptide peptidase (SPP)²². In this report, we define three additional HLA-A2-restricted T cell epitopes derived from either the hydrophobic core region (h-region) of the ppCT signal peptide (ppCT_{9–17}) or the procalcitonin (pCT) precursor protein (ppCT_{50–59} and ppCT_{91–100}). They are processed in the cytosol after release of a peptide precursor from the ppCT leader

sequence by SPP or after retrotranslocation of a pCT substrate from the endoplasmic reticulum (ER) lumen by the ER-associated degradation (ERAD) pathway, respectively. Importantly, active immunotherapy based on a cocktail of five ppCT peptides, including ppCT_{16–25}, ppCT_{9–17} and a 15-amino acid (aa)-long peptide derived from the NH₂-terminal region of the ppCT leader sequence (ppCT_{1–15}), was able to induce antitumour CTL responses in HLA-A*0201/HLA-DR3-transgenic (HHD-DR3) mice and NOD-*scid-Il2ry^{null}* (NSG) mice adoptively transferred with human peripheral blood mononuclear cells (PBMCs), capable of controlling growth of established tumours expressing low levels of HLA-A2/human ppCT peptide complexes. We propose that ppCT leader sequence-derived peptides constitute promising T cell targets permitting CTL to eradicate tumours with impaired antigen processing and presenting machinery (APM) and thus overcome tumour escape from CD8 T cell immunity.

Results

ppCT and TAP expression in human lung tumours. To further extend our previous studies²² on the prevalence of *CALCA* gene expression in primary human lung tumours, we first evaluated the level of the *calcitonin* (*CT*) transcript in tumours from 28 additional non-small-cell lung carcinoma (NSCLC) patients and allogeneic normal thyroids, used as a reference, by quantitative real-time PCR (qRT-PCR). High expression levels of *CT* mRNA were detected in several lung cancer samples as compared to allogeneic thyroid tissues (Table 1). Indeed, up to 39% of lung tumour tissues, mainly from adenocarcinoma (ADC) histological subtypes, (over)expressed the *CT* transcript, with levels ranging from 2- to 2,000-fold higher than those found in normal human thyroids. We then confirmed the expression of *CT* at the protein level by immunohistochemistry (IHC) in a cohort of 215 formalin-fixed paraffin-embedded (FFPE) lung tumour samples (Supplementary Figure 1a), where up to 20% of ADC and 38% of neuroendocrine tumours (NET) expressed the protein (Table 2).

Our previous studies had demonstrated that downregulation of TAP1 or TAP2 subunits potentiates ppCT_{16–25} epitope presentation on tumour cells expressing the *CALCA* gene²³. We therefore evaluated the prevalence of TAP downregulation in human lung cancer specimens by analysing the expression levels of *TAP1* and *TAP2* mRNA in primary human tumours and autologous normal lungs. qRT-PCR studies indicated that up to 71% of the 28 analysed lung tumours expressed low levels of *TAP1* and/or *TAP2* mRNA as compared to autologous normal lungs (Table 1). To estimate the percentage of tumours with TAP protein defects, we performed IHC staining with anti-TAP2 mAb in a cohort of 135 FFPE lung tumour samples (Supplementary Figure 1b). Results indicated that 53% and 32% of the tumours displayed low and intermediate expression levels of TAP2, respectively, while only 14% of human lung tumours expressed high levels of the TAP2 subunit (Table 3). These results suggest that immunotherapy based on the ppCT precursor protein may help to overcome tumour escape from CD8 T cell immunity associated with TAP subunit expression defects.

Selection of HLA-A2-binding peptides derived from the ppCT.

Next, we asked whether ppCT includes additional HLA-A*0201-restricted epitopes that could trigger an antitumour CTL response. With this aim, we screened the entire sequence of the ppCT precursor for the presence of peptides with high binding affinity for HLA-A*0201 using the epitope prediction software SYFPEITHI. We selected two peptides, ppCT_{9–17} and ppCT_{50–59}, with high predicted binding scores and derived from the hydrophobic central region (h-region) of the ppCT signal peptide and the pCT prohormone, respectively (Table 4). We also selected

Table 1 Relative expression of CT and TAP transcripts in lung tumour samples

Histological type	Tumour sample	Relative expression of CT transcript	Relative expression of TAP1 transcript	Relative expression of TAP2 transcript
ADC	ADC-1	0.18	0.26	0.47
	ADC-2	1.24	1.24	1.61
	ADC-3	92.41	2.18	2.71
	ADC-4	2112.89	0.44	0.63
	ADC-5	13.32	2.03	0.9
	ADC-6	2.11	0.57	0.46
	ADC-7	368.37	0.07	0.08
	ADC-8	1.69	2.68	1.34
	ADC-9	5.96	0.29	0
	ADC-10	0.27	0.75	0.48
	ADC-11	652.58	0.74	0.93
	ADC-12	0.53	0.08	0.1
	ADC-13	3.68	0.53	0.15
	ADC-14	0.41	1.46	2.53
LCC	LCC-1	0.65	0	0.06
	LCC-2	1.74	1.98	0.76
	LCC-3	0.17	0.41	0.65
	LCC-4	0	0.21	0.3
	LCC-5	1.27	0	0
SCC	SCC-1	747.02	7.26	8
	SCC-2	3.13	0.18	0.16
	SCC-3	4.16	0	0
	SCC-4	0.64	0.17	0.27
	SCC-5	0.2	0.03	0.01
	SCC-6	0	0.05	0.11
NET	NET-1	0.29	0.05	0.05
	NET-2	0.84	0.33	0.42
	NET-3	0.17	0.03	0.09

qRT-PCR analysis of CT and TAP transcripts in fresh human lung tumour samples. Normalized copy numbers of CT and TAP transcripts are shown. The expression of CT was normalized to allogeneic healthy thyroid tissues, and expression of TAP was normalized to autologous healthy lung tissue. Values of the CT transcript that are statistically elevated are shown in bold and those of TAP that are statistically downregulated are shown in bold and italics ($P < 0.001$ according to the Mann-Whitney U test)

NET neuroendocrine tumours, ADC adenocarcinomas, LCC large cell carcinomas, SCC squamous cell carcinomas

Table 2 Expression of CT protein in lung tumours

Histological type	Low	Medium	High	Percentage
ADC (67 samples)	5	7	1	20%
SCC (35 samples)	0	0	0	0%
NET (58 samples)	7	6	9	38%
Undif (47 samples)	2	2	0	9%
Other (8 samples)	0	1	1	25%
Total	14/215	16/215	11/215	19%/215

Calcitonin (CT) protein expression in a cohort of 215 FFPE lung tumour samples was performed by IHC

NET neuroendocrine tumours, ADC adenocarcinomas, SCC squamous cell carcinomas, Undif undifferentiated

additional peptides, such as ppCT₅₋₁₄, ppCT₄₁₋₄₉, ppCT₅₃₋₆₂, ppCT₈₇₋₉₆ and ppCT₉₁₋₁₀₀, with a predicted binding score higher than or similar to that of ppCT₁₆₋₂₅ (Table 4, Supplementary Table 1).

We then evaluated the capacity of all the selected peptides to bind to HLA-A*0201 and to form stable HLA-A*0201/peptide complexes using the TAP-deficient HLA-A2-transfected T2 cell line. Similarly to the mutated E27L MelanA/Mart-1₂₆₋₃₅ epitope, used as a positive control^{24,25}, ppCT₅₀₋₅₉, ppCT₄₁₋₄₉ and ppCT₉₋₁₇ peptides and, to a much lesser extent, ppCT₉₁₋₁₀₀,

displayed high binding affinity and stabilization capacity towards HLA-A*0201, fulfilling the characteristics of immunogenic peptides²⁶ (Table 4). In contrast, other peptides with high predictive scores, such as ppCT₅₋₁₄, ppCT₅₃₋₆₂ and ppCT₈₇₋₉₆, were excluded because they displayed very low binding affinity towards HLA-A*0201 (Supplementary Table 1). These results suggest that the ppCT preprohormone includes at least two additional HLA-A2-restricted epitopes that may induce a CD8 T cell response.

ppCT₉₋₁₇, ppCT₅₀₋₅₉ and ppCT₉₁₋₁₀₀ are immunogenic epitopes. To determine whether the identified ppCT peptides are immunogenic, we first analysed their capacity to activate specific human CD8⁺ T lymphocytes in vitro. For this purpose, we twice stimulated, at 1-week intervals, lung cancer patient PBMCs with each of the four peptides and then evaluated generation of ppCT-specific CTLs by intracellular IFN- γ staining or the enzyme-linked immunospot (Elispot) assay. The ppCT₄₁₋₄₉ peptide was rapidly excluded because it was not immunogenic in any of the five patient and healthy donor PBMCs tested. Among HLA-A2⁺ patients tested by intracellular staining (see Supplementary Figure 2a), 8 out of 13, 10 out of 15 and 7 out of 15 patients triggered IFN- γ -producing CD8⁺ T cells towards ppCT₉₋₁₇, ppCT₅₀₋₅₉ and ppCT₉₁₋₁₀₀ peptides, respectively (Fig. 1a, b). The ppCT₁₆₋₂₅ and MelanA/Mart-1₂₆₋₃₅ epitopes, included as positive controls, induced specific IFN- γ -producing CD8⁺ T cells in 5 out of 15 and 6 out of 13 patient PBMCs, respectively (Fig. 1a, b). Induction of specific IFN- γ -producing cells was also observed in some PBMCs from HLA-A2⁺ healthy donors (Supplementary Figure 1b and Fig. 1c). Moreover, Elispot assay confirmed induction of peptide-specific IFN- γ -producing cells in PBMCs isolated from several NSCLC patients among the 28 additional patients tested (Fig. 1d, e). These results indicate that lung cancer patients respond 2.5- to 3.5-fold more frequently to ppCT peptides than healthy donors (Supplementary Figure 2c).

We then addressed the question of whether ppCT₉₋₁₇, ppCT₅₀₋₅₉ and ppCT₉₁₋₁₀₀ were naturally processed by tumour cells by testing the capacity of responding T cell lines to recognize the ppCT^{high}TAP^{low} IGR-Heu cell line generated from patient 1 (Heu) and the IGR-Heu-TAP cell line, which we had previously transfected with TAP1/2-encoding plasmids²³. In agreement with our previous studies²³, CTL induced towards ppCT₁₆₋₂₅ lysed the parental IGR-Heu tumour cell line more efficiently than the TAP-transfected target (Fig. 2a). In contrast, ppCT₉₋₁₇, ppCT₅₀₋₅₉ and ppCT₉₁₋₁₀₀-specific CTL displayed stronger cytotoxic activity towards TAP-efficient than towards TAP-deficient tumour cells. Cytotoxicity towards IGR-Heu and IGR-Heu-TAP target cells was inhibited by anti-MHC-I mAb (W6/32), indicating that it is most likely TCR mediated (Fig. 2a). Peptide specificity was further confirmed using HLA-A2⁺ Epstein-Barr virus (EBV)-transformed B cells generated from patient 1 (Heu-EBV), unpulsed or pulsed with each of the peptides (Supplementary Figure 3a). Results indicated that CD8⁺ T cells generated towards ppCT peptides more efficiently killed specific peptide-loaded B cells than unloaded B cells. In contrast, they were unable to kill the natural killer-sensitive target cell line K562, further supporting the conclusion that cytotoxicity towards IGR-Heu tumour cells is specific and TCR mediated (Supplementary Figure 3a). Moreover, cytotoxicity towards the IGR-Heu-TAP tumour cell line was inhibited by adding an excess of competing unlabelled target cells pulsed with ppCT₉₋₁₇, ppCT₅₀₋₅₉ or ppCT₉₁₋₁₀₀ peptide (Supplementary Figure 3b). We then generated, from patient 1, several T cell clonoids and T cell clones towards each of the ppCT epitopes and measured IFN- γ production upon stimulation with autologous IGR-Heu and IGR-Heu-TAP

Table 3 Expression of TAP2 protein in lung tumours

Histological type	Low	Intermediate	High
ADC (56 samples)	22/56 (39%)	25/56 (45%)	9/56 (16%)
SCC (29 samples)	20/29 (69%)	7/29 (24%)	2/29 (7%)
Undif (42 samples)	24/42 (57%)	10/42 (24%)	8/42 (19%)
Other (8 samples)	6/8 (75%)	2/8 (25%)	0/8 (0%)
Total	72/135 (53%)	44/135 (32%)	19/135 (14%)

TAP2 protein expression in a cohort of 135 FFPE lung tumour samples was performed by IHC. Data correspond to TAP2 H-score. Low: $0 \leq H\text{-score} \leq 70$; Intermediate: $80 \leq H\text{-score} \leq 140$; High: $160 \leq H\text{-score} \leq 200$. H-score = % TAP2⁺ cells × TAP2 intensity. TAP2 intensity varies from 0 to 2. Normal cell H-score = 200
ADC adenocarcinomas, SCC squamous cell carcinomas, Undif undifferentiated

Table 4 Identification of HLA-A2-restricted ppCT epitopes

Peptide	aa Sequence	SYFPEITHI prediction	FI	DC ₅₀ (h)
ppCT ₉₋₁₇	FLALSILVL	28	1.27	5
ppCT ₁₆₋₂₅	VLLQAGSLHA	18	0.24	3
ppCT ₅₀₋₅₉	LLAALVQDYL	24	2.58	10
ppCT ₉₁₋₁₀₀	CMLGTYTQDF	12	0.30	4
E27L Mart- ₁₂₆₋₃₅	ELAGIGILTV	28	3.03	8

Fixation and stabilization assays were performed with 100 μM of a given peptide. FI (fluorescence index) = (mean fluorescence intensity (MFI) with the given peptide – MFI without peptide)/MFI without peptide; DC₅₀: half-life of the HLA-A2-peptide complexes
aa amino acid

tumour cell lines. Data showed that, while T cell cloids generated towards ppCT₉₋₁₇, ppCT₅₀₋₅₉ and ppCT₉₁₋₁₀₀ epitopes produced higher levels of IFN-γ when stimulated with IGR-Heu-TAP, T cell clones generated towards the ppCT₁₆₋₂₅ epitope produced higher cytokine levels when stimulated with autologous IGR-Heu tumour cells (Fig. 2b). Notably, CTL generated towards ppCT-derived peptides also killed, with variable killing efficiency, the TAP-proficient ppCT⁺ medullary thyroid carcinoma (MTC) cell line TT (Supplementary Figure 3c). Thus ppCT₉₋₁₇, ppCT₁₆₋₂₅, ppCT₅₀₋₅₉ and ppCT₉₁₋₁₀₀ epitopes appear to be more immunogenic in NSCLC patients than in healthy donors and are naturally processed in ppCT-expressing tumour cells.

Processing of ppCT₉₋₁₇, ppCT₅₀₋₅₉ and ppCT₉₁₋₁₀₀ epitopes.

The above results suggested that ppCT₉₋₁₇, ppCT₅₀₋₅₉ and ppCT₉₁₋₁₀₀ epitopes are processed by a TAP-dependent mechanism. Therefore, we examined the involvement of the proteasome/TAP pathway in ppCT peptide processing using the proteasome inhibitor epoxomicin and small interference RNA (siRNA) targeting TAP1. Results indicated that epoxomicin inhibited the cytotoxicity of ppCT₉₋₁₇, ppCT₅₀₋₅₉ and ppCT₉₁₋₁₀₀-specific CTL towards IGR-Heu-TAP tumour cells (Fig. 3a). In contrast, it induced a slight increase in the cytotoxicity of ppCT₁₆₋₂₅-specific CTLs generated from patient 1. Epoxomicin also inhibited IFN-γ release by ppCT₉₋₁₇, ppCT₅₀₋₅₉ and ppCT₉₁₋₁₀₀-specific T cell cloids stimulated with IGR-Heu-TAP tumour cells, while it had only a marginal effect on IFN-γ release by ppCT₁₆₋₂₅-specific T cell clones stimulated with IGR-Heu (Fig. 3b). As expected, downregulation of TAP1 in IGR-Heu-TAP tumour cells resulted in an increase in their susceptibility to anti-ppCT₁₆₋₂₅ CTL-mediated lysis, while it resulted in a decrease in anti-ppCT₉₋₁₇, anti-ppCT₅₀₋₅₉, anti-ppCT₉₁₋₁₀₀ and CTL-mediated killing (Supplementary Figure 4a).

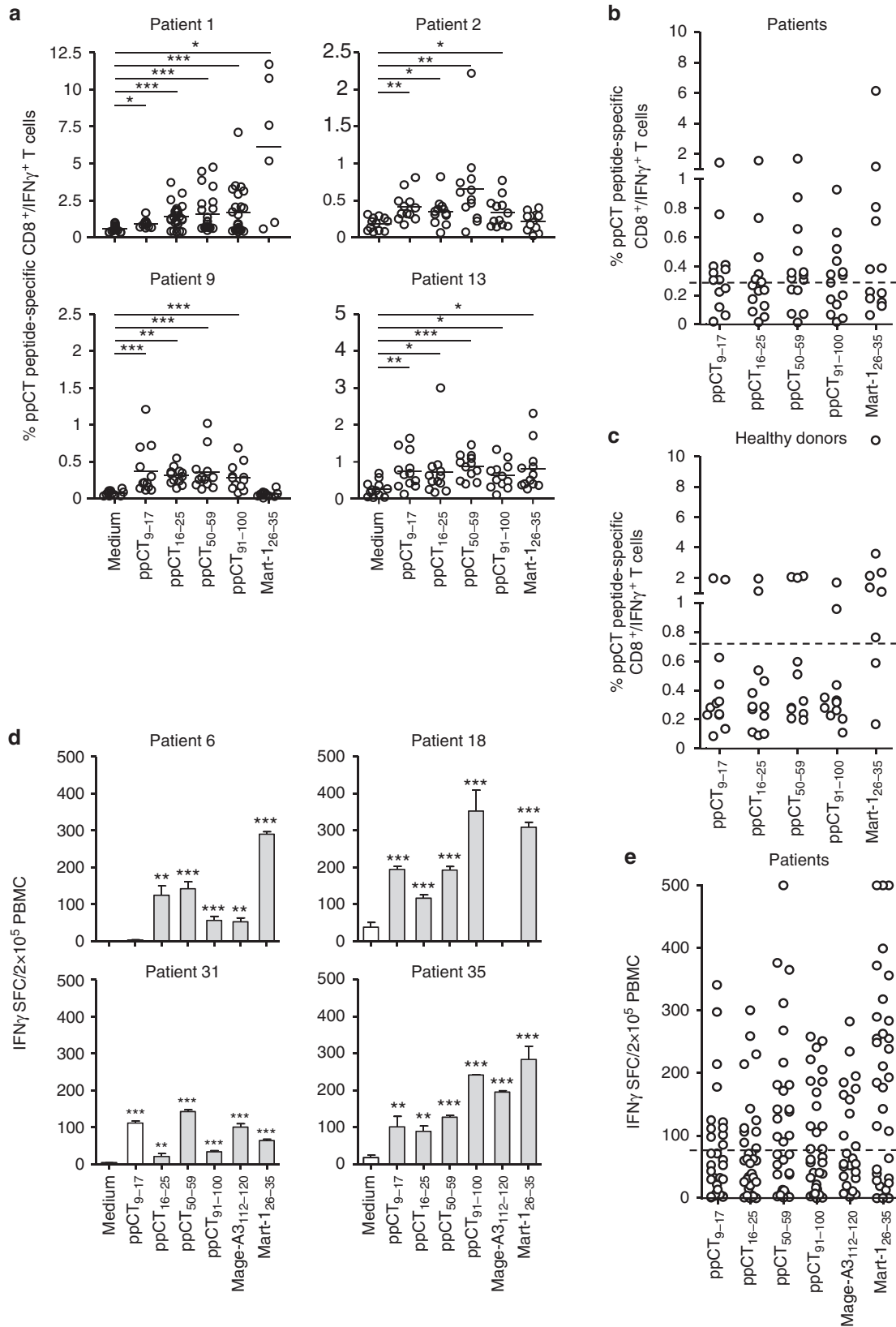
Because the ppCT₉₋₁₇ peptide is part of the ppCT signal sequence²⁷, it is presumably dependent on SP. Accordingly, preincubation of IGR-Heu-TAP with the serine protease inhibitor

dichloroisocoumarin (DCI)²⁸ markedly inhibited cytotoxicity of CD8⁺ T cells generated towards ppCT₉₋₁₇, as well as ppCT₅₀₋₅₉ and ppCT₉₁₋₁₀₀ (Fig. 3c). DCI also inhibited IFN-γ release of all ppCT peptide-specific T cell cloids and clones generated from patient 1 and stimulated with autologous IGR-Heu-TAP or IGR-Heu tumour cells (Fig. 3b). The involvement of SPP in the processing of ppCT₉₋₁₇ was then demonstrated using specific siRNA, which inhibited lysis of CTL generated towards the ppCT₉₋₁₇ epitope (Fig. 3d). These results indicate that cleavage of the ppCT signal peptide by SP is required for further processing of all ppCT epitopes. They also suggest that, after cleavage by SPP, a ppCT₁₋₁₇ signal peptide fragment is released into the cytoplasm to be further processed by the proteasome and that the generated ppCT₉₋₁₇ peptide is then translocated to the ER lumen by TAP. Accordingly, further downregulation of TAP1 in IGR-Heu tumour cells using specific siRNA (Supplementary Figure 4b) induced a decrease in the lytic activity of ppCT₉₋₁₇ epitope-specific CTLs (Supplementary Figure 4c).

We next examined the role of the ERAD pathway in processing of the pCT precursor protein by treating IGR-Heu and IGR-Heu-TAP tumour cells with the eeyarstatin 1 (EER1) inhibitor. Results included in Fig. 3e show that EER1 inhibited target cell killing by anti-ppCT₅₀₋₅₉ and anti-ppCT₉₁₋₁₀₀ CTLs, while it had only a marginal effect on ppCT₉₋₁₇ and ppCT₁₆₋₂₅-specific CTLs. In these experiments, we verified that DCI, epoxomicin, EER and siRNA targeting SPP and TAP1 had no or only a weak effect on tumour cell viability (Supplementary Figure 4d) and cell surface expression of HLA-A2 molecules (Supplementary Figure 4e). These results indicate that the pCT prohormone undergoes retrotranslocation from the ER into the cytosol to be processed by the proteasome/TAP pathway. The generated ppCT₅₀₋₅₉ and ppCT₉₁₋₁₀₀ epitopes, as well as the ppCT₉₋₁₇ epitope, are then loaded into the ER on HLA-A2 molecules to be presented at the target cell surface.

ppCT triggers CTL responses towards APM-impaired tumours.

Synthetic long peptides constitute a promising vaccine strategy for inducing therapeutic T cell responses in patients with tumours. Therefore, we selected from the ppCT precursor protein two 15-aa-long peptides, ppCT₁₋₁₅ and ppCT₈₆₋₁₀₀, each of which included at least three additional peptides predicted to bind to HLA-A2 (ppCT₂₋₁₀, ppCT₄₋₁₂ and ppCT₇₋₁₅ and ppCT₈₇₋₉₅, ppCT₉₂₋₁₀₀ and ppCT₉₁₋₉₉, respectively; see Supplementary Table 1). These 15-aa-long peptides induced specific IFN-γ-secreting CD8⁺ T cells in PBMCs from 7 out of 10 and 5 out of 10 NSCLC patients, respectively (Fig. 4a, b). We then identified a cocktail of five peptides, including the three ppCT leader sequence-derived peptides (ppCT₁₋₁₅, ppCT₉₋₁₇ and ppCT₁₆₋₂₅), ppCT₅₀₋₅₉ and ppCT₈₆₋₁₀₀, able to induce strong CD8⁺ T cell responses in a majority of patient PBMCs, as monitored by IFN-γ production (Fig. 4c) and killing of IGR-Heu and IGR-Heu-TAP tumour cells (Fig. 4d).



Next, we tested whether the selected ppCT peptide cocktail could prime ppCT-specific CTLs capable of controlling growth of APM-impaired tumours in vivo. Initial experiments performed in HHD-DR3 transgenic mice immunized with each of the HLA-A2-restricted epitopes, co-administered with the TLR3 agonist

polyinosinic-polycytidylic acid (poly(I:C)) adjuvant, showed that ppCT₉₋₁₇ and ppCT₅₀₋₅₉ induce peptide-specific IFN- γ -producing cells in the spleens of immunized mice (Supplementary Figure 5a). In contrast, dimethyl sulphoxide (DMSO) alone or combined with poly(I:C) had no effect on cytokine production

Fig. 1 Immunogenicity of ppCT-derived epitopes in NSCLC patient PBMCs. **a** Cytoplasmic expression of IFN- γ in CD8⁺ T cells as determined by cytoplasmic immunofluorescence analysis. PBMCs were stimulated for 14 days in 96-well plates with the indicated peptides or with medium (containing DMSO alone), then restimulated for 6 h in the same conditions, as described in Methods. Cells from eight culture wells (one column) were pooled and then stained with anti-CD8 mAb, and after membrane permeabilization, they were stained with anti-IFN- γ mAb. For each peptide, 12–15 columns were included. For media and control peptides, six columns were tested for patients for whom insufficient amounts of PBMCs were available. Samples were analysed using an Accuri C6 cytometer, and data were processed by the Cflow software. Circles correspond to the percentages of positive cells in one column from a 96-well plate. Horizontal lines correspond to mean percentages of positive cells. Data shown are from 4 patients out of 15. * $p < 0.05$; ** $p < 0.01$; *** $p < 0.001$ (two-tailed Mann-Whitney U test). **b** Mean percentages of IFN- γ -producing CD8⁺ T cells from 15 analysed NSCLC patients' PBMCs. The horizontal dashed line corresponds to the cutoff value (e.g. mean of the medium condition mean values plus 2 times the SD) above which responses are considered positive. **c** Mean percentages of IFN- γ -producing CD8⁺ T cells from 12 analysed healthy donors' PBMCs. The horizontal dashed line corresponds to the cutoff value above which responses are considered positive. **d** IFN- γ SFC from NSCLC patients' PBMCs. PBMCs from NSCLC patients were stimulated in 96-well plates with the indicated peptides (24 culture wells for each peptide) as described in **a**; then cells were pooled, and IFN- γ -secreting cells were evaluated by Elispot assay. Values correspond to means (\pm SD) of SFC from triplicates. Data shown are from 4 patients out of 28. ** $p < 0.01$; *** $p < 0.001$ (two-tail Student's unpaired t test with Welch's correction). **e** Means of IFN- γ SFC from 28 patients' PBMCs. The horizontal dashed line corresponds to the cutoff value above which responses are considered positive. HLA-A2-restricted Mart-1_{26–35} and/or Mage-A3_{112–120} (KVAELVHFL) peptides were included as controls. SFC spot-forming cells

(Supplementary Figure 5b). Moreover, the induced CD8⁺ T cells were able to trigger cytotoxic activity towards IGR-Heu-TAP and/or IGR-Heu tumour cells that was inhibited by anti-MHC-I mAb (Supplementary Figure 5c). Results also indicated that mice immunized with the cocktail of five ppCT peptides administered together with poly(I:C) adjuvant (hereafter named ppCT active immunotherapy or therapeutic ppCT peptide vaccine) developed specific CD8⁺ T cells able to produce IFN- γ when restimulated ex vivo either with specific peptides alone, mainly ppCT_{1–15}, ppCT_{9–17} and ppCT_{50–59}, or with the peptide cocktail (Fig. 5a). Cytotoxicity of the induced ppCT-specific T cells was also examined in vivo 2 days after the last immunization with the ppCT peptide vaccine following injection of syngeneic splenocytes loaded with the peptide cocktail. Strong killing activity towards specific ppCT peptide-loaded splenocytes, but not towards MART-1_{26–35} peptide-loaded splenocytes used as a control, was seen 24 h after target cell administration, supporting the role of ppCT-specific CTLs in controlling tumour progression (Fig. 5b).

We then examined the antitumour response of the ppCT-based vaccine formulation in HHD-DR3 mice engrafted with the weakly immunogenic D122 clone of Lewis lung carcinoma cell line LL2, transgenic for HLA-A2 (D122-HHD) and transfected with a human ppCT-encoding lentivirus (D122-HHD-ppCT; Supplementary Figure 5d), expressing intermediate levels of HLA-A2 molecules (Supplementary Figure 5e). Results indicated that D122-HHD-ppCT tumours grew much more slowly in vaccinated than in non-vaccinated (DMSO plus poly (I:C)) mice (Fig. 5c, d). Moreover, control of tumour growth in vaccinated mice was correlated with much stronger tumour infiltration with T lymphocytes than in non-vaccinated mice (Fig. 5e). To further assess the capacity of ppCT-based immunotherapy to control progression of APM-impaired human tumours, we developed a preclinical model of NSG mice engrafted with the human ppCT⁺ IGR-Heu tumour, expressing low levels of HLA-A2 (Supplementary Figure 5e), and then adoptively transferred with human healthy donor PBMCs previously tested in vitro for their capacity to induce a T cell response towards ppCT epitopes. Data showed a delay in tumour growth in mice treated with ppCT peptide vaccine compared to mice treated with DMSO plus poly (I:C) control (Fig. 5f, g). Moreover, an increase in the absolute number of human CD8⁺ T cells producing IFN- γ when restimulated ex vivo with the peptide cocktail was observed in tumour-infiltrating lymphocytes (TILs) from vaccinated mice as compared to non-vaccinated mice (Fig. 5h). Overall, these data indicate that ppCT peptide-based active immunotherapy triggers an efficient antitumour T cell response towards APM-impaired

tumours and that it corresponds to a promising strategy for treatment of ppCT-expressing tumours that have escaped conventional immunotherapies.

Discussion

In the present study, we report on T lymphocytes specific to the ppCT tumour antigen and on CD8-T cell-defined ppCT-derived epitopes processed by proteasome/TAP-independent and -dependent mechanisms. We also report here that human lung tumours frequently express the ppCT precursor protein and that most of them display defects in TAP1 and/or TAP2 expression. Deficiencies in TAP subunits have been described in several human cancer types, including cervical²⁹, head and neck³⁰, melanoma and gastric^{31–33} cancers, and were associated with tumour escape from CD8 T cell immunity. Thus CTLs specific for such antigen-processing mutants and their target antigens have been identified for use in preventing cancer immune evasion and designing more effective anticancer therapeutic strategies. Interestingly, most of these CTLs were found to recognize epitopes derived from signal peptides of precursor proteins that are independent of cytosolic processing and transport pathways^{34–36}. Among rare known epitopes belonging to this class of antigens are the human HLA-A2-restricted melanoma-associated tyrosinase 1–9 epitope³⁷, the ppCT_{16–25} epitope^{22,23} and the murine H2-D^b-restricted C-terminal peptide epitope of TRH4 ceramide synthase³⁸. While the human ppCT_{16–25} epitope is derived from the C-terminal region of the preprotein signal peptide and is processed by the SP and SPP pathway²², the murine TRH4 epitope is generated by SPP independently of the SP³⁸.

After cleavage by SPP, signal peptide fragments can be released either into the ER, where they follow TAP-independent processing³⁹, i.e. the ppCT_{16–25} epitope²², or into the cytoplasm, to be processed by the proteasome/TAP pathway, i.e. signal peptide-derived epitopes presented by HLA-E molecules⁴⁰. Here we provide evidence that the ppCT signal peptide generates an additional HLA-A2-restricted epitope, ppCT_{9–17}, the processing of which is dependent not only on SP (required to release the leader sequence from the precursor protein) but also on SPP and presumably also TAP. These results are in agreement with the observation that signal sequences that have been cleaved by SP can be further processed by SPP and then by cytosolic proteases³⁹. In *Escherichia coli*, cleaved signal sequences are processed by membrane-bound protease IV and further degraded by cytosolic oligopeptidase⁴¹. In eukaryotic cells, processing of signal peptide fragments can also occur in the cytosol⁴² and then bind to MHC-I molecules in the ER lumen^{43–45}. Likewise, the ppCT signal peptide is cleaved by SPP to generate the ppCT_{16–25} epitope

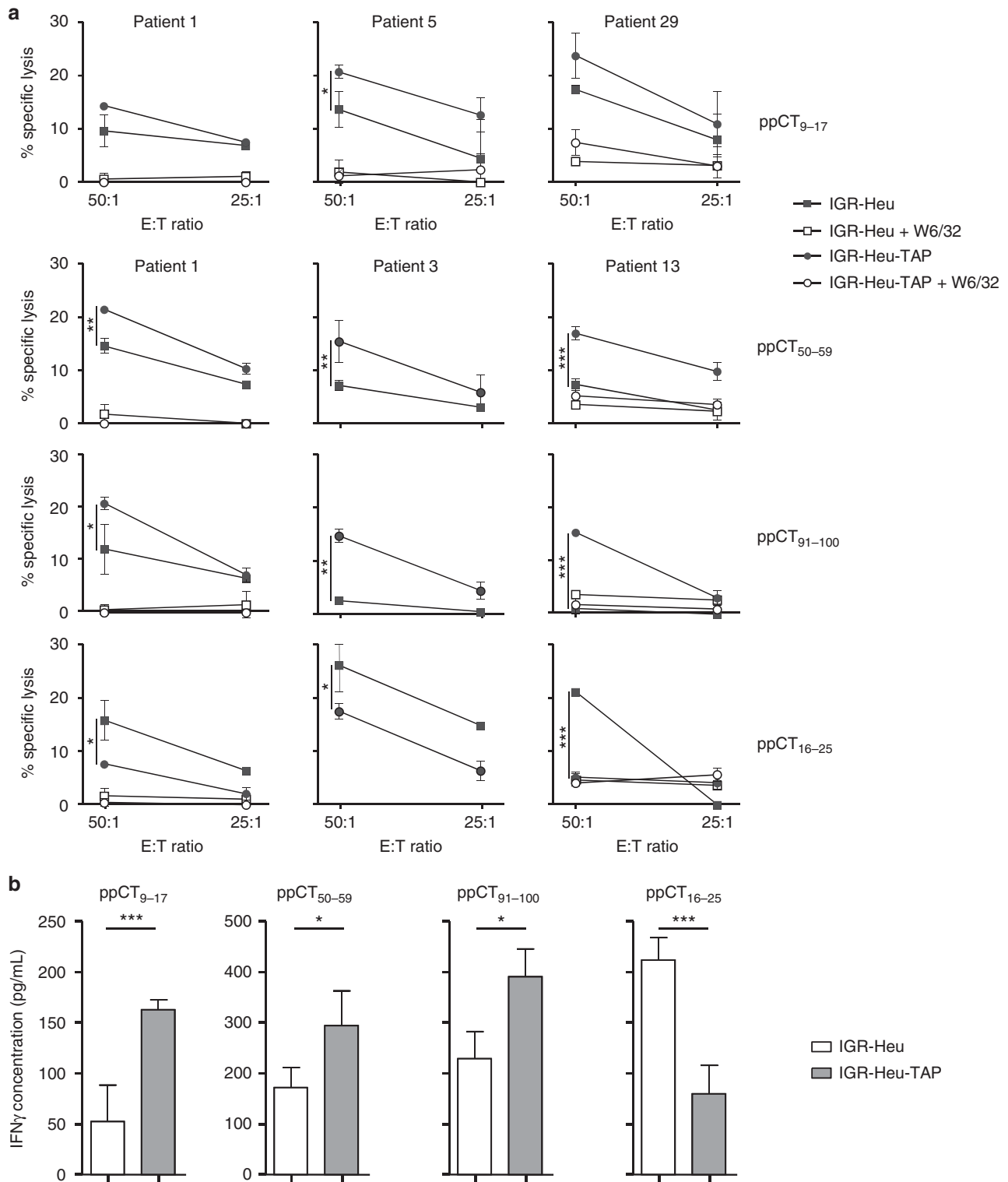
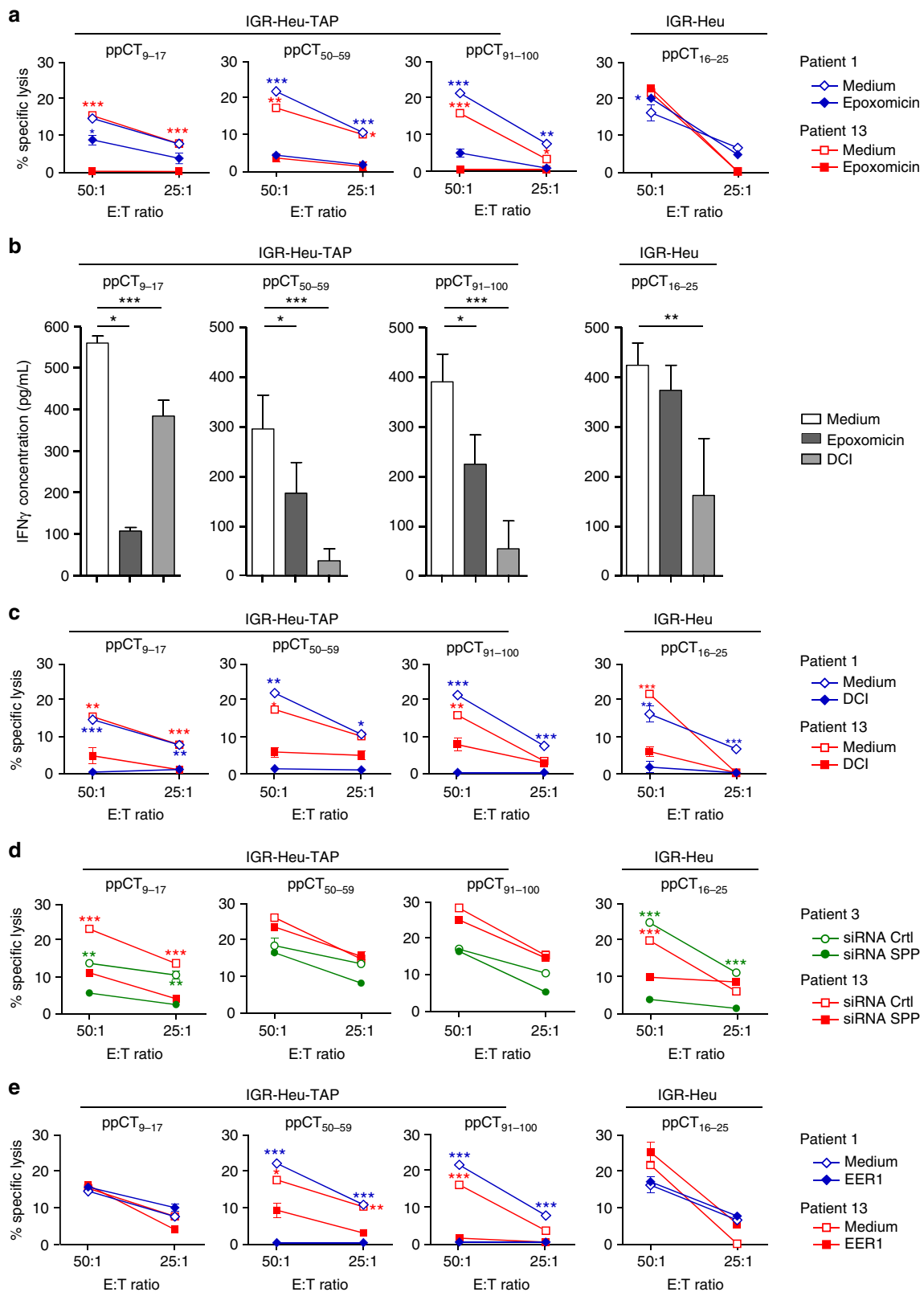


Fig. 2 Specificity of ppCT-peptide-stimulated CD8⁺ T cells. **a** NSCLC patient PBMCs were stimulated in vitro with the indicated peptides, and then CD8⁺ T cells were isolated and their cytotoxic activity was tested. The IGR-Heu and IGR-Heu-TAP (IGR-Heu transfected with TAP1 and TAP2) tumour cell lines, generated from patient 1 (Heu), pre-incubated or not with neutralizing anti-MHC-I mAb W6/32, were used as targets. Cytotoxicity was determined by a conventional 4-h ⁵¹Cr release assay at the indicated E:T ratios. Values correspond to means (±SD) of percentages of lysis from triplicates. Data shown represent experiments from three patients' PBMCs. **b** Cytokine release of patient 1's T cell clones and T cell clonoids stimulated with the autologous IGR-Heu and IGR-Heu-TAP cell lines. IFN-γ release was measured using ELISA. Data shown are means (±SD) of three T cell clones and three T cell clonoids from three independent experiments. **p* < 0.05; ****p* < 0.001 (two-tailed Student's unpaired *t* test). E:T effector:target



within the ER, and a ppCT₁₋₁₇ peptide, which is released into the cytosol, to be further processed by the proteasome to generate the ppCT₉₋₁₇ epitope, which is then likely translocated to the ER lumen by TAP. Therefore, fragments from leader sequences with a type II signal anchor³⁹, like the ppCT signal peptide^{22,46}, are released into the ER lumen and presented to CTLs by MHC-I

molecules in a TAP-independent manner (such as the ppCT₁₆₋₂₅ epitope) or into the cytosol where they are further processed by the proteasome (like the ppCT₁₋₁₇ peptide). Thus it makes sense that the resulting fragments (such as the ppCT₉₋₁₇ epitope) would be transported by TAP into the ER lumen, where they bind to the MHC-I molecules and then conveyed to the cell surface to be

Fig. 3 Processing pathway of the ppCT₉₋₁₇, ppCT₅₀₋₅₉ and ppCT₉₁₋₁₀₀ epitopes. **a** Processing of pCT₉₋₁₇, ppCT₅₀₋₅₉ and ppCT₉₁₋₁₀₀ peptides is proteasome dependent. IGR-Heu or IGR-Heu-TAP cells were incubated in the absence or presence of the proteasome inhibitor epoxomicin, and then the generated epitope-specific CTLs were added. Cytotoxic activity was determined by the ⁵¹Cr-release assay at the indicated E:T ratios. Values correspond to means (±SD) of percentages of lysis from triplicates. **b** Production of IFN-γ by patient 1's T cell clones or cloids stimulated with autologous ppCT-expressing tumour cell lines. Anti-ppCT peptide T cells were stimulated for 36 h with IGR-Heu-TAP (anti-ppCT₉₋₁₇, -ppCT₅₀₋₅₉ and -ppCT₉₁₋₁₀₀) or IGR-Heu (anti-ppCT₁₆₋₂₅) tumour cells, untreated or pretreated with epoxomicin or DCI; then IFN-γ production was measured by ELISA. Data shown are means (±SD) of three T cell clones and T cell cloids from three independent experiments. **c** Involvement of SP in processing of ppCT₉₋₁₇, ppCT₅₀₋₅₉ and ppCT₉₁₋₁₀₀ antigenic peptides. IGR-Heu-TAP tumour cells were incubated with SP inhibitor DCI before addition of anti-ppCT epitope CTLs. Cytotoxicity of anti-ppCT₁₆₋₂₅ CTLs towards IGR-Heu tumour cells, untreated or pretreated with DCI, was included. **d** Processing of the ppCT₉₋₁₇ epitope involves SPP. The lytic activity of ppCT₉₋₁₇, ppCT₅₀₋₅₉- and ppCT₉₁₋₁₀₀-specific CTLs against IGR-Heu-TAP, electroporated with siRNA targeting SPP (siRNA SPP) or siRNA control (siRNA Ctrl), was examined as in **a**. **e** Processing of ppCT₅₀₋₅₉- and ppCT₉₁₋₁₀₀ epitopes is ERAD dependent. IGR-Heu and IGR-Heu-TAP tumour cells were incubated in the absence or presence of EER1, and then epitope-specific CTLs were added. Values correspond to means (±SD) of percentage of lysis from triplicates. Data shown are from two independent experiments out of three. **p* < 0.05; ***p* < 0.01; ****p* < 0.001 (two-tailed Student's unpaired *t* test). Blue: patient 1, red: patient 13 and green: patient 3. DCI dichloroisocoumarin, EER1 eeyarestatin 1, E:T effector:target

recognized by CTLs. Generation of both ppCT₁₆₋₂₅ and ppCT₉₋₁₇ epitopes by SPP supports the hypothesis that the cleavage site of this aspartic protease in the centre of the h-region of the ppCT signal peptide is approximate and may lead to different peptide fragments. The ppCT₉₋₁₇ epitope is most likely naturally processed by tumour cells, since the generated CTL were able to lyse ppCT-expressing target cells.

Apart from its leader sequence, ppCT can also generate HLA-A2-restricted CTL epitopes from the N-terminal region of pre-protein (ppCT₅₀₋₅₉) or the hormone itself (ppCT₉₁₋₁₀₀). Their processing also requires cleavage of the signal peptide by SP and the ERAD pathway, which involves substrate retrotranslocation from the ER lumen into the cytosol for degradation by the proteasome/TAP pathway. Indeed, after cleavage of its signal peptide, with type II orientation, i.e. spanning the ER membrane with the n-region exposed towards the cytosol and the c-region facing the ER lumen^{22,46}, pCT is released into the ER, where it is subsequently transferred across the membrane, via ERAD⁴⁷⁻⁴⁹, to enter the cytosol and then follow proteasome/TAP-dependent processing. Accordingly, processing of ppCT₅₀₋₅₉ and ppCT₉₁₋₁₀₀ is inhibited not only by DCI but also by EER1 and epoxomicin, which inhibit SP, ERAD and proteasome, respectively. These results support the conclusion that release of the signal peptide is a prerequisite for further processing of the preprotein, which can occur either in the ER by the SP/SPP pathway (ppCT₁₆₋₂₅) or in the cytosol after cleavage by SPP (ppCT₉₋₁₇) or retranslocation of the pCT from the ER lumen via the ERAD pathway (ppCT₅₀₋₅₉ and ppCT₉₁₋₁₀₀).

Identification of TAA in solid tumours, in particular, melanoma, led to development of therapeutic peptide-based cancer vaccines, the aim of which is to activate or reactivate tumour-specific CTLs. Therapeutic peptide vaccinations with TAA, including differentiation antigens, overexpressed antigens, cancer/testis antigens and viral antigens, are currently under investigation, and results are promising⁵⁰. Transfer of in vitro-activated TILs^{8,9} and blockade of inhibitory receptors such as CTLA-4 and PD-1 have led to impressive results, with survival benefits in many cancers, including NSCLC³⁻⁶. Success of cancer immunotherapies, including cancer vaccines, has been associated with (re)activation of T lymphocytes specific to neoantigens arising from DNA mutations in tumour cells^{8,9,12-17}. Unfortunately, only a subset of patients responds to these therapies, indicating that tumours are able to use additional resistance mechanisms to escape immunotherapy-induced antitumour T cell responses. Among these mechanisms, alterations in tumour APM play an important role. In this context, it has been shown that defects in the HLA-class I APM may occur in malignant cells after active immunotherapy⁵¹ and PD-1 blockade immunotherapy²⁰. Some of these defects include an irreversible tapasin

mutation associated with loss of HLA genes, a truncating mutation in the gene encoding β2m and loss of TAP subunits⁵²⁻⁵⁷. Thus self-antigens belonging to TEIPP are particularly attractive because they emerge on cancer cells with defects in APM and thus enable overcoming tumour escape from CD8 T cell immunity.

The ppCT-based immunotherapy that we have developed here includes at least one TEIPP (ppCT₁₆₋₂₅), two additional peptides derived from the ppCT signal peptide (ppCT₉₋₁₇ and ppCT₁₋₁₅) and two peptides derived from the pCT (ppCT₅₀₋₅₉ and ppCT₈₆₋₁₀₀). Inclusion of proteasome/TAP-independent and -dependent HLA-A2-restricted epitopes would enable targeting cancer cells with either an impaired or functional proteasome/TAP pathway and thus overcoming tumour evasion from CTL attack. Moreover, the ppCT-based therapeutic vaccine includes two 15-aa-long peptides (ppCT₁₋₁₅ and ppCT₈₆₋₁₀₀) that would permit activating CD8⁺ and possibly CD4⁺ ppCT-specific T lymphocytes. This active cancer immunotherapy, delivered with the TLR3-ligand poly(I:C) as adjuvant, resulted in pronounced progression delay of lung tumours displaying impaired APM established in HLA-A2 transgenic mice or NSG mice that were adoptively transferred with healthy donor PBMCs. Tumour growth control was associated with induction of ppCT-specific CD8⁺ T cells, including ppCT₁₆₋₂₅ TEIPP-specific T cells. TEIPP-specific T lymphocytes were also found to be activated by therapeutic vaccination with synthetic long peptides composing the minimal CD8 T cell epitope²¹. These results suggest that TAP-proficient host antigen-presenting cells were able to process these long peptides and to cross-present TEIPP in MHC-I molecules, in the context of a fully competent peptide repertoire.

Overall, our findings provide in vitro and in vivo proof of concept of a ppCT-based therapeutic cancer vaccine and support the conclusion that signal sequence-derived peptides and their carrier proteins are attractive candidates for specific active cancer immunotherapy. They also provide a rational design of combinatorial cancer immunotherapy harnessing a ppCT-based peptide vaccine, together with checkpoint inhibitors, in particular anti-PD-1 and anti-PD-L1 mAbs, to treat patients suffering from NSCLC, MTC and NET and to prevent outgrowth of immune-escaped cancer cells.

Methods

Healthy volunteers and patients. Healthy donor blood samples were collected from the French blood bank (Etablissement Français du Sang (EFS); agreement number No. 12/EFS/079), and patient samples were collected from Gustave Roussy. All patients were suffering from advanced and inoperable NSCLC stage IIIB/IV. Blood samples were drawn from patients after induction chemotherapy. Immune monitoring in the blood of patients was approved by the Kremlin-Bicêtre Hospital Ethics Committee (no. 110-08; ID RCB: 2008-A01171-54), and Declaration of Helsinki protocols were followed. Healthy donors and patients provided their written informed consent prior to inclusion in this study.

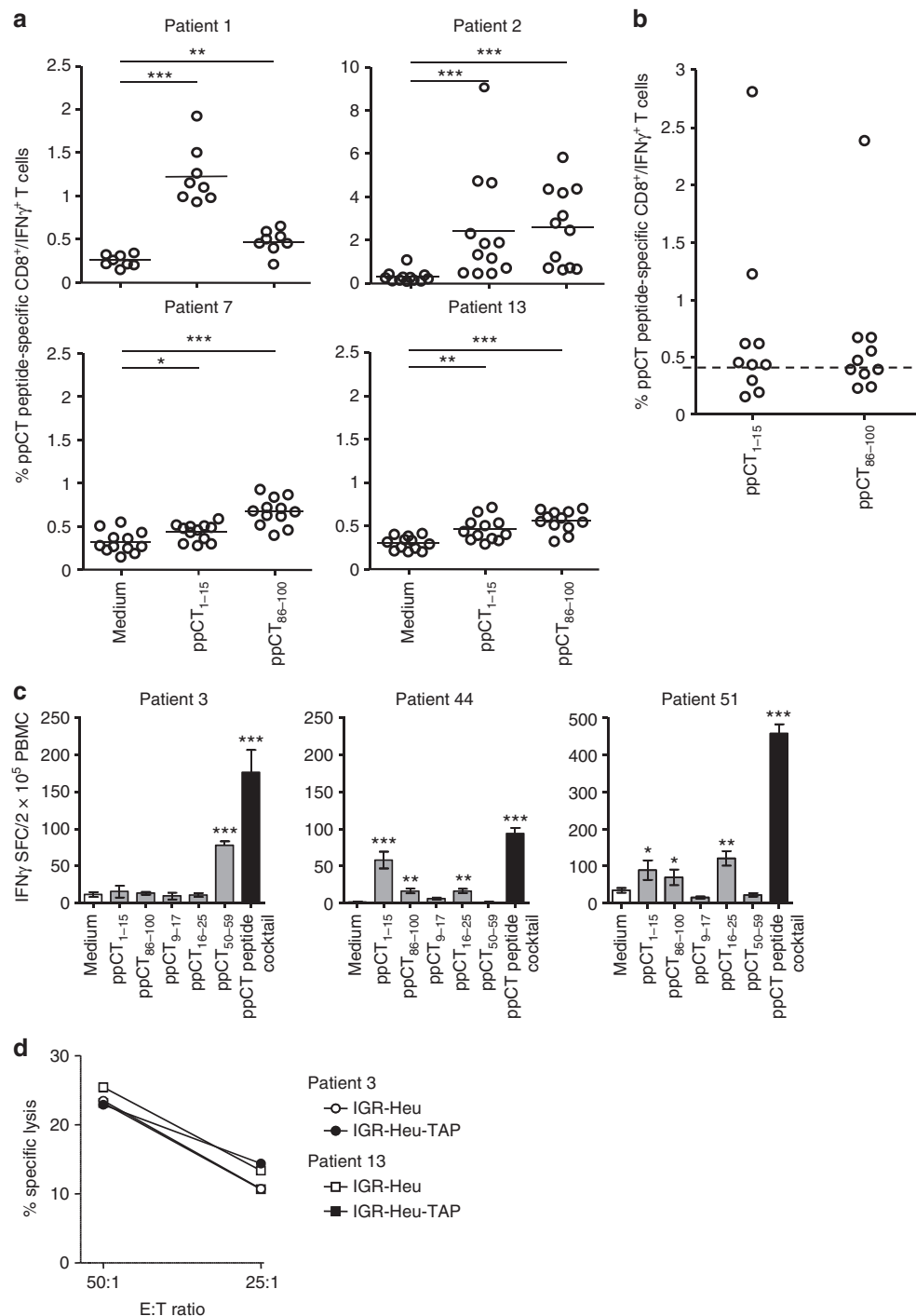


Fig. 4 Immunogenicity of ppCT 15-aa-long peptides and a peptide cocktail in patients' PBMCs. **a** Cytoplasmic expression of IFN- γ in CD8⁺ T cells as determined by intracellular immunofluorescence analysis. NSCLC patients' PBMCs were stimulated with ppCT₁₋₁₅ or ppCT₈₆₋₁₀₀ peptides, then surface-labelled with anti-CD8 mAb and cytoplasmic-labelled with anti-IFN- γ mAb. Percentages of positive cells from 4 patients' PBMCs are included. * p < 0.05; ** p < 0.01; *** p < 0.001 (two-tailed Mann-Whitney U test). **b** Mean percentages of IFN- γ -producing CD8⁺ T cells from 10 analysed NSCLC patients' PBMCs. The horizontal dashed line corresponds to the cutoff value (e.g. mean of the medium condition mean values plus 2 times the SD) above which responses are considered positive. **c** IFN- γ -producing CD8⁺ T cells. PBMCs from NSCLC patients were stimulated with the indicated peptides or the peptide cocktail; then IFN- γ SFC were evaluated by Elispot assay. Values correspond to means (\pm SD) of SFC from triplicates. Data shown are from three patients. * p < 0.05; ** p < 0.01; *** p < 0.001 (two-tail Student's unpaired t test with Welch's correction). **d** Cytotoxicity of ppCT peptide cocktail-specific CD8⁺ T cells towards IGR-Heu and IGR-Heu-TAP tumour cells. Values correspond to means (\pm SD) of percentages of lysis from triplicates. Data shown represent experiments from two patients. SFC spot-forming cells, E:T effector:target

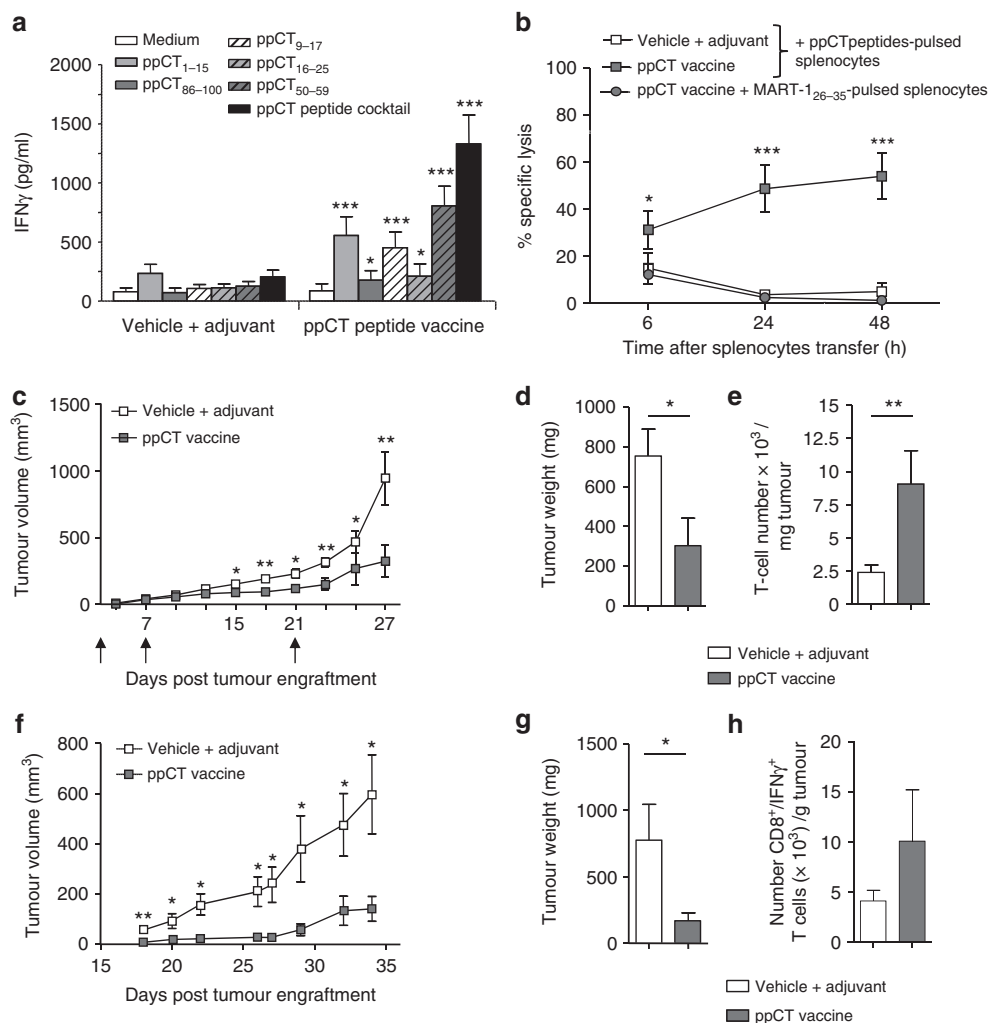


Fig. 5 Immunogenicity and antitumour effect of ppCT vaccine. **a** In vivo immunogenicity in HHD-DR3 mice. Mice were immunized four times at 1-week intervals with the ppCT vaccine or vehicle plus adjuvant control. One week after the final immunization, splenocytes were recovered and cultured in medium or restimulated with each peptide or the peptide cocktail; then IFN- γ secretion was measured. Three-to-five mice per group were included. Results are means (\pm SEM) of three independent experiments ($n = 12$). **b** In vivo cytotoxic activity. Splenocytes were loaded with ppCT peptides and injected i.v. 2 days after the last immunization. Surviving target cell frequencies were detected in blood 6, 24 and 48 h later. Five mice per group were included. Results are means (\pm SEM) of two independent experiments ($n = 10$). **c** Tumour progression. 10^6 D122-HHD-ppCT cells were injected s.c. At days 1, 7 and 21 (arrows), mice were vaccinated with ppCT vaccine or vehicle plus adjuvant and tumour volume was measured every third day. **d** Tumour weight. Tumours were recovered at day 27 after engraftment and weighed. **e** Absolute TIL counts. Numbers of TILs per milligram of tumour. Three-to-five mice per group were included. Results in **c–e** are given as means (\pm SEM) of four independent experiments ($n = 16$). **f** IGR-Heu tumour growth in NSG mice. NSG mice were engrafted with IGR-Heu tumour pieces and, at day 10, adoptively transferred with healthy donor PBMCs. At days 11 and 17, mice were vaccinated i.v. with the ppCT vaccine or with vehicle plus adjuvant, and tumour growth was recorded every 2 days. **g** Tumour weight. Tumours were recovered at day 34 after engraftment and weighed. Bars are mean \pm SEM. Results are from one experiment out of six. **h** Absolute number of human IFN- γ -producing CD8 $^+$ T cells. Tumours were recovered, dissociated and human CD45 $^+$ leukocytes were isolated and restimulated with the ppCT peptide cocktail. Total number of IFN- γ -producing CD3 $^+$ CD8 $^+$ cells was determined. Five mice per group were included. Results in **f–h** are means (\pm SEM) of one experiment out three ($n = 16$). * $p < 0.05$; ** $p < 0.01$; *** $p < 0.001$ (two-tailed Student's unpaired t test)

Real-time qRT-PCR and IHC staining. Fresh NSCLC tumours and normal lung tissues of 32 patients were obtained from the Centre chirurgical Marie Lannelongue and the Institut Mutualiste Montsouris. RNA were immediately extracted with TRIZOL reagent (Invitrogen), reverse-transcribed and then subjected to qRT-PCR²². RNAs from a pool of five human healthy thyroid tissues⁵⁸ were included. PCR probes for *TAP1*, *TAP2* and *CALCA* genes were designed by Applied Biosystems (*TAP1*: Hs00184465_m1; *TAP2*: Hs00241066_m1; *CALCA*: Hs00266142_m1) and used according to the manufacturer's recommendations.

FFPE primary tumour samples were obtained from patients diagnosed with early-stage NSCLC⁵⁹. A total of 215 tumour samples, including 31% ADC, 16% squamous cell carcinomas, 27% NET, 22% undifferentiated tumour and 4% other subtypes were tested by IHC for CT expression using anti-CT (Dako, ref. A0576, dilution 1/2000) Ab. From this cohort, a total of 135 FFPE tumour samples were tested by IHC for TAP protein expression using anti-TAP2 Ab (dilution 1/20) produced in one of our laboratories⁶⁰. Briefly, 4- μ m-thick whole sections from

FFPE lung cancer specimens were mounted on poly-L-lysine-coated slides, deparaffinized and rehydrated through graded alcohol to water. Antigen retrieval was performed in a citrate buffer (pH = 6) for 30 min at 98 °C. Endogenous peroxidase activity was inhibited with 3% hydrogen peroxidase (Sigma Aldrich) for 10 min, and non-specific proteins were blocked for 15 min. The primary Ab was incubated for 1 h at room temperature (RT). Immunostaining was visualized using goat anti-rabbit horseradish peroxidase (HRP) 1:100 (Powersvision, Leica, ref. PV6119) for 20 min at RT and then adding 3,3'-diaminobenzidine substrate (Powersvision, Leica). Slides were counterstained with Mayer's haematoxylin (VWR).

Antibodies and immunofluorescence analyses. Anti-human CD8-APC (ref. 130-091-076, dilution 1/100) and anti-IFN- γ -PE (ref. 130-113-493, dilution 1/50) mAbs were purchased from Miltenyi Biotec. Anti-human CD45-PE-Cy7 (ref. 25-0459-42, dilution 1/200), anti-CD3-FITC (ref. 11-0038-42, dilution 1/200),

anti-CD4-PE (ref. 12–0048–42, dilution 1/200), anti-IFN- γ -APC (ref. 17–7319–82, dilution 1/100) and anti-mouse anti-CD8-alexafluor 700 (ref. 56–0081–82, dilution 1/200) mAbs were purchased from ThermoFisher Scientific. Anti-human CD8-Pacific-Blue (ref. 301026, dilution 1/200) and anti-mouse CD3-APC-Cy7 (ref. 100222, dilution 1/200) mAbs were provided by Biolegend. Anti-HLA-A2 (BB7.2 and MA2.1, dilutions 1/1000 and 1/400, respectively) and anti-MHC-I (W6/32, dilution 1/100) mAbs were purified from ascitic fluids in one of our laboratories.

Expression of surface molecules was performed by immunofluorescence analyses using specific mAb. For cytoplasmic IFN- γ expression, human PBMCs were stimulated for 6 h at 37 °C with 2.5 μ M of each peptide in the presence of 10 μ g/ml Brefeldin A (Sigma, ref. B6542). After anti-CD8 staining, cells were fixed with phosphate-buffered saline (PBS) containing 2% formaldehyde; their membrane was permeabilized using PBS supplemented with 0.5% bovine serum albumin and 0.2% saponin and then stained with anti-IFN- γ mAb. Samples were analysed using an Accuri C6 cytometer or Fortessa cell analyser (BD Biosciences), and data were processed by the Cflow software (BD Biosciences) or FlowJo software (Tree Star Inc).

Peptide prediction, HLA-A*0201 binding and stability assays. The ppCT sequence was scanned for HLA-A*0201-binding peptides using the prediction software SYFPEITHI (www.syfpeithi.de). Three 9–10-aa-long peptides, ppCT_{9–17} (FLALSILVL), ppCT_{50–59} (LLAALVQDYL) and ppCT_{91–100} (CMLGTYTQDF), were selected from a ppCT signal peptide (ppCT_{9–17}) and pCT (ppCT_{50–59} and ppCT_{91–100}) precursor protein. Two 15-aa-long peptides, ppCT_{1–15} (MGFQKFSPLALSIL) and ppCT_{86–100} (GNLSTCMLGTYTQDF), were also selected because they include additional predicted HLA-A2-restricted peptides. Peptides were synthesized by Genescript or Proteogenix at a purity of >75%. Lyophilized peptides were dissolved in DMSO at a concentration of 10–100 mM and stored at –80 °C.

To determine whether the candidate peptides can bind to HLA-A*0201, upregulation of peptide-induced HLA-A2 molecule expression on T2 cells (ATCC® CRL-1992™) was examined. Briefly, 3 × 10⁵ T2 cells were incubated with 100 μ M of the synthesized peptides and 100 ng/ml of human β 2m (β 2m, Sigma) in serum-free RPMI 1640 medium for 16 h at 37 °C. T2 cells incubated with β 2m alone served as a negative control. Expression of HLA-A*0201 on T2 cells was then examined by staining with BB7.2 mAb, followed by fluorescein isothiocyanate (FITC)-labelled goat-anti-mouse IgG (Biolegend, ref. 405305, dilution 1/100) secondary Ab. The fluorescence index (FI) was calculated as follows: FI = (mean fluorescence intensity (MFI) with the given peptide – MFI without peptide)/MFI without peptide⁶¹. The HLA-A2.1-restricted Melan-A/MART-1_{26–35} peptide served as positive control⁶².

To test peptide/HLA-A*0201 complex stability, T2 cells were incubated at 37 °C overnight with 100 μ M of each peptide in serum-free RPMI 1640 medium supplemented with 100 ng/ml of β 2m and washed to remove free peptides. They were then incubated with 10 μ g/ml of brefeldin A for 1 h to block newly synthesized HLA-A*0201 molecules from being expressed on the cell surface, washed and incubated at 37 °C for 30 min, 1, 2, 4, 6, 8 or 12 h. Subsequently, cells were stained with BB7.2 mAb and FITC-labelled goat anti-mouse IgG. For each peptide, the equation of linear trend line was determined and the half-life (DC₅₀) of the HLA-A2-peptide complex was calculated.

In vitro T cell stimulation with synthetic peptides. For induction of peptide-specific CTLs, PBMCs were isolated using Ficoll-Paque and incubated for 1 h at 37 °C with 20 μ M of each peptide in RPMI medium supplemented with 1% human AB serum (SAB). Peptide-pulsed PBMCs were washed and plated at 2 × 10⁵ cells/0.2 ml in U-bottom 96-microwell plates, in RPMI medium with 10% SAB, 1% sodium pyruvate, penicillin (100 U/ml), streptomycin (10 μ g/ml), IL-2 (20 U/ml, Miltenyi Biotech, ref. 130–097–745), IL-4 (10 ng/ml, Miltenyi Biotech, ref. 130–093–922) and IL-7 (10 ng/ml, Miltenyi Biotech, ref. 130–095–363). At day 7, cells were restimulated with the same medium supplemented with 20 μ M peptide, and 1 week later, each microplate column was harvested and T cell functional activities were analysed. T cell clones and T cell clonals specific to ppCT peptides were generated from patient 1 by limiting dilution^{63–65}.

Functional assays. IFN- γ secretion was measured using Ready-Set-Go enzyme-linked immunosorbent assay (ELISA) according to the manufacturer's recommendation (eBioscience, ref. 88–7316). Briefly, 96-well plates were coated overnight with anti-mouse or anti-human IFN- γ mAb (capture Ab) at 4 °C. Then plates were washed with PBS–Tween 20 and saturated for 1 h. Supernatants were diluted to 1/10, transferred to plates and incubated for 2 h at RT. After washing, plates were further incubated with biotinylated anti-mouse IFN- γ mAb (detection Ab) for 1 h at RT. Plates were washed, incubated for 30 min at RT with avidin-HRP and then developed by the addition of substrate solution (TMB), followed by 10–15 min of incubation at RT in the dark. The enzymatic colour development was stopped by addition of sulphuric acid solution (2 N), and the optical densities of each well were read at 450 and 570 nm using a microplate reader (Opsys MR, Dynex Technologies). The values of 570 nm were subtracted from those of 450 nm and data were analysed. IFN- γ concentrations in supernatants were determined from the standard curve and expressed as pg/ml.

The peptide-specific T cell response induced after *in vitro* stimulation of patient PBMCs with ppCT-derived peptides was examined using the Elispot assay according to the manufacturer's recommendation (Diacclone, Elispot, ref. 856.051). Briefly, 96-well plates containing nitrocellulose filters (Multiscreen; Millipore) were coated overnight with anti-IFN- γ mAbs (capture Ab) at 4 °C. The plates were washed with PBS–Tween 20 and saturated for 2 h with RPMI medium, 10% SAB. One week after the last stimulation, PBMCs were cultured in triplicate at 2 × 10⁵ cells/well and restimulated with peptides at 20 μ M. For positive control, PBMCs were stimulated with 1 ng/ml phorbol myristate acetate (PMA) and 500 ng/ml ionomycin. After 16 h, plates were washed with PBS–Tween 20 and incubated for 10 min at 4 °C. Plates were then washed with PBS–Tween 20 and incubated for 1 h 30 min with biotinylated anti-mouse IFN- γ and 1 h with alkaline-phosphatase-conjugated streptavidin. Spots were developed by adding phosphatase substrates, 5-bromo-4,3-indolyl phosphate/nitroblue tetrazolium (BCIP/NBT) and spot-forming cells (SFC) were counted using the CTL Immunospot system (Cellular Technology Ltd). Cells stimulated with PMA (1 ng/ml, Sigma, ref. P1582) and ionomycin (500 ng/ml, Sigma, ref. I0634) were included as positive controls. The negative control consisted of cells cultured in medium alone. A response was considered positive if the number of spots in the well containing cells stimulated with peptides was at least 2-fold higher than the number of spots in the well containing cells without peptide, with a cutoff of 10 SFC.

In vitro T cell cytotoxicity activity was measured by a conventional 4 h chromium (⁵¹Cr) release assay⁶⁶. CD8⁺ T cells, isolated by magnetic beads using the CD8⁺ T Cell Isolation Kit (Miltenyi Biotech, ref. 130–096–495), and T cell clones and clonoids were used as effector cells. For proteasome, SP and ERAD inhibition, 10⁶ tumour cells were resuspended in media in the presence of specific inhibitors. Briefly, tumour cells were incubated for 2 h at 37 °C with epoxomicin (10 μ M, Merck Millipore, ref. 324800), DCI (250 μ M, Merck Millipore, ref. 287815) or EERI (10 μ M, Merck Millipore, ref. 324521)^{67,68}, washed, resuspended in acid buffer for 30 s, washed and then incubated for an additional 3 h in the presence of each inhibitor. None of the inhibitors were toxic at the given concentrations, as tested by the Annexin V Apoptosis Detection Kit I (BD Pharmingen, ref. 556547). The parental tumour cell line IGR-Heu, TAP1- and TAP2-transfected cell line IGR-Heu-TAP, generated from patient 1 (Heu)²³, the lymphoblastoid B cell line Heu-EBV (established in one of our laboratories) and human erythroleukaemia cell line K562 (ATCC® CCL-243™) were used as targets. All the cell lines are mycoplasma-free and were regularly tested for mycoplasma contamination. We regularly authenticate IGR-Heu and IGR-Heu-TAP cell lines by testing recognition by autologous CTL clones, such as ppCT-specific clones, and HLA-A2 and TAP expression. Gene silencing of SPP (HMI13, sense 5'-gac aug ccu gaa aca aca dtdt-3', and antisense 5'-uga uug uuu cagg caug uc dtdg-3', Ambion, ref. 202377) and TAP1 (HS_TAP1_2_HP, sense 5'-gcc gau acc uuc acu cga a dtdt-3' and antisense 5'-uuc gag uga agg uau cgg c dtdg-3', Qiagen, ref. SI00012418) expression in IGR-Heu target cells was performed using sequence-specific siRNA^{22,23}.

Mice, in vivo experiments and immunization protocol. HHD-DR3 (mice humanized for both HLA-A2 and HLA-DR3 and deleted for both H-2 class I and 2 molecules (β 2m –/– H-2Db –/– I α B –/– I α A –/– I ϵ β –/–)) and NSG mice were bred and maintained at the animal facility of Gustave Roussy. Animal experiments were performed in accordance with guidelines established by the institutional animal committee (CEEA no. 26: 2012–146 and 2017–081–12717). Eight-to-12-week-old male and female HHD-DR3 transgenic mice, randomized to obtain homogeneous groups in term of gender and age, were immunized subcutaneously (s.c.) with equimolar amounts of peptides (100 μ M) emulsified in poly (I:C) adjuvant (Invivogen, ref. vac-pic). One week after the last immunization, cell suspensions from the spleens were cultured for 3 days in RPMI medium supplemented with 20 μ M of peptides and 20 U/ml of IL-2, and then IFN- γ secretion was tested by ELISA (ebioscience, ref. 88–7314).

In vivo cytotoxic activity was measured using the VITAL assay^{69,70}. Briefly, HHD-DR3 splenocytes were incubated for 2 h either in the presence of DMSO alone, with 10 μ M MART-1_{26–35} negative control or with 0.1 or 10 μ M ppCT peptide cocktail, and then labelled with 0.5 or 5 μ M CellTrace™ Far Red (Molecular Probes, ref. C34564) for non-specifically-loaded (MART-1_{26–35}) and unloaded (DMSO) targets, respectively, or with 0.1 or 1 μ M carboxyfluorescein succinimidyl ester (CFSE; Molecular Probes, ref. C34554) for 10 and 0.1 μ M of ppCT-specific loaded targets, respectively. Labelled cells were mixed at equal ratios and 3 × 10⁶ cells of each population were injected intravenously (i.v.) at 6, 24 and 48 h after target cell injection and blood was collected for flow cytometric analysis. The percentage of specific killing was calculated with the following formula: 100 – [100 × (% CFSE⁺ cells in mice vaccinated/% Far red⁺ cells in vaccinated mice)/(mean of % CFSE⁺ cells in non-vaccinated mice/mean of % Far red⁺ cells in non-vaccinated mice)].

For the antitumour response, HHD-DR3 mice were inoculated s.c. with 1 × 10⁶ of Lewis lung carcinoma D122-HHD-ppCT cells (Lewis lung carcinoma transgenic for HLA-A2, a gift from L Eisenbach, Weizmann Institute, Israel and infected with a lentivirus encoding ppCT in one of our laboratories) and then vaccinated s.c. at days 1, 7 and 21 after tumour engraftment. Tumour volume was measured using a caliper twice a week and estimated using the following formula: length × width × thickness (mm³). At day 27, tumours were surgically removed, weighed and dissociated by enzymatic digestion according to the manufacturer's recommendations (Tumour Dissociation Kit, Miltenyi Biotech, ref. 130–096–730).

T lymphocytes from each tumour were then positively selected using anti-CD90.2 mAb-coated Dynabeads according to the standard immunoselection protocol (DynaL, Invitrogen, ref. 11465D). Single-cell suspensions were counted, the percentage of CD3⁺/CD8⁺ lymphocytes was determined by flow cytometry and the number of TILs per milligram of tumour was then calculated.

An immunodeficient mouse model that can be used to analyse the human CTL response to ppCT-based active immunotherapy was developed and adapted from refs. 71,72 in accordance with guidelines established by the institutional animal committee (CEEA no. 26: 2012–147 and 2017–081–12717). With this aim, 6–10-week-old male and female NSG mice, randomized to obtain homogeneous groups in term of gender and age, were engrafted s.c. with the patient 1 tumour (Heu-n-IR), which was generated by implantation of the IGR-Heu tumour cell line previously transfected with the intercellular adhesion molecule-1 adhesion molecule and CCL5 (Rantes) chemokine in one of our laboratories, and maintained in nude mice⁷³. When tumours were palpable, about 10 days later, mice were injected i.v. with 2×10^7 healthy donor PBMCs. Before transfer into mice, healthy donor PBMCs were tested in vitro for their capacity to induce a CD8 T cell response towards ppCT epitopes. At days 1 and 7 after PBMC engraftment, mice were vaccinated i.v. with the ppCT peptide vaccine, and tumour volume was measured every 2 days as described above. Tumours were recovered at day 28 after engraftment, weighed and dissociated as described above. Human CD45⁺ leukocytes were then selected by magnetic beads (Miltenyi Biotech, ref. 130–045–801), restimulated for 6 h with allogeneic HLA-A2* mature dendritic cell pulsed with the ppCT peptide cocktail, and the number of human CD3⁺/CD8⁺ cells secreting IFN- γ per gram of tumour was determined by flow cytometry. In this study, approximately 250 mice were used and divided in groups of 5–10 mice per group. Animals were randomized to obtain homogeneous groups in term of gender and age.

Statistical analyses. The sample size for in vitro and in vivo experiments were determined by calculation of the statistical power. GraphPad Prism5 software (GraphPad Software, Inc., San Diego, CA, USA) was used for graphic representation and statistical analysis. For in vitro experiments, a two-tailed Mann–Whitney *U* test was applied to statistically analyse the efficiency of ppCT peptides at generating CD8⁺/IFN- γ ⁺ T lymphocytes after stimulation of NSCLC patient PBMCs. A two-tailed Student's unpaired *t* test with Welch's correction (we do not assume equal variances) was applied to analyse the specific precursor number after peptide stimulation of NSCLC patient PBMCs. A two-tailed Student's unpaired *t* test was applied to determine peptides processing. Mean \pm error bars (standard deviation, SD) was shown. For in vivo experiments, a two-tailed Student's paired *t* test was used to statistically analyse the immunogenicity of the ppCT peptide vaccine. A two-tailed Student's unpaired *t* test was used for statistical analysis of the antitumour effect of the ppCT peptide vaccine. Mean \pm error bars (standard error of the mean, SEM) is shown.

Data availability

A reporting summary for this article is available as Supplementary Information file. The authors state that all data generated during this study are included in the article and its supplementary information file and are available from the corresponding author upon reasonable request.

Received: 8 February 2017 Accepted: 30 October 2018

Published online: 30 November 2018

References

- Hinrichs, C. S. & Rosenberg, S. A. Exploiting the curative potential of adoptive T-cell therapy for cancer. *Immunol. Rev.* **257**, 56–71 (2014).
- Barrett, D. M., Grupp, S. A. & June, C. H. Chimeric antigen receptor- and TCR-modified T cells enter Main Street and Wall Street. *J. Immunol.* **195**, 755–761 (2015).
- Hodi, F. S. et al. Improved survival with ipilimumab in patients with metastatic melanoma. *N. Engl. J. Med.* **363**, 711–723 (2010).
- Mellman, I., Coukos, G. & Dranoff, G. Cancer immunotherapy comes of age. *Nature* **480**, 480–489 (2011).
- Wolchok, J. D. et al. Nivolumab plus ipilimumab in advanced melanoma. *N. Engl. J. Med.* **369**, 122–133 (2013).
- Sharma, P. & Allison, J. P. Immune checkpoint targeting in cancer therapy: toward combination strategies with curative potential. *Cell* **161**, 205–214 (2015).
- Tumeh, P. C. et al. PD-1 blockade induces responses by inhibiting adaptive immune resistance. *Nature* **515**, 568–571 (2014).
- Lu, Y. C. et al. Efficient identification of mutated cancer antigens recognized by T cells associated with durable tumor regressions. *Clin. Cancer Res.* **20**, 3401–3410 (2014).
- Tran, E. et al. Cancer immunotherapy based on mutation-specific CD4⁺ T cells in a patient with epithelial cancer. *Science* **344**, 641–645 (2014).
- Robbins, P. F. et al. Mining exomic sequencing data to identify mutated antigens recognized by adoptively transferred tumor-reactive T cells. *Nat. Med.* **19**, 747–752 (2013).
- Cohen, C. J. et al. Isolation of neoantigen-specific T cells from tumor and peripheral lymphocytes. *J. Clin. Invest.* **125**, 3981–3991 (2015).
- Snyder, A. et al. Genetic basis for clinical response to CTLA-4 blockade in melanoma. *N. Engl. J. Med.* **371**, 2189–2199 (2014).
- Van Allen, E. M. et al. Genomic correlates of response to CTLA-4 blockade in metastatic melanoma. *Science* **350**, 207–211 (2015).
- Rizvi, N. A. et al. Cancer immunology. Mutational landscape determines sensitivity to PD-1 blockade in non-small cell lung cancer. *Science* **348**, 124–128 (2015).
- McGranahan, N. et al. Clonal neoantigens elicit T cell immunoreactivity and sensitivity to immune checkpoint blockade. *Science* **351**, 1463–1469 (2016).
- Pritchard, A. L. et al. Exome sequencing to predict neoantigens in melanoma. *Cancer Immunol. Res.* **3**, 992–998 (2015).
- Carreno, B. M. et al. Cancer immunotherapy. A dendritic cell vaccine increases the breadth and diversity of melanoma neoantigen-specific T cells. *Science* **348**, 803–808 (2015).
- Gao, J. et al. Loss of IFN- γ pathway genes in tumor cells as a mechanism of resistance to anti-CTLA-4 therapy. *Cell* **167**, 397–404 e399 (2016).
- Shin, D. S. et al. Primary resistance to PD-1 blockade mediated by JAK1/2 mutations. *Cancer Discov.* **2**, 188–201 (2016).
- Zaretsky, J. M. et al. Mutations associated with acquired resistance to PD-1 blockade in melanoma. *N. Engl. J. Med.* **375**, 819–829 (2016).
- Doorduyn, E. M. et al. TAP-independent self-peptides enhance T cell recognition of immune-escaped tumors. *J. Clin. Invest.* **126**, 784–794 (2016).
- El Hage, F. et al. Preprocalcitonin signal peptide generates a cytotoxic T lymphocyte-defined tumor epitope processed by a proteasome-independent pathway. *Proc. Natl. Acad. Sci. USA* **105**, 10119–10124 (2008).
- Durgeau, A. et al. Different expression levels of the TAP peptide transporter lead to recognition of different antigenic peptides by tumor-specific CTL. *J. Immunol.* **187**, 5532–5539 (2011).
- Ayyoub, M. et al. Activation of human melanoma reactive CD8⁺ T cells by vaccination with an immunogenic peptide analog derived from Melan-A/melanoma antigen recognized by T cells-1. *Clin. Cancer Res.* **9**, 669–677 (2003).
- Romero, P. et al. Antigenicity and immunogenicity of Melan-A/MART-1 derived peptides as targets for tumor reactive CTL in human melanoma. *Immunol. Rev.* **188**, 81–96 (2002).
- van der Burg, S. H., Visseren, M. J., Brandt, R. M., Kast, W. M. & Melief, C. J. Immunogenicity of peptides bound to MHC class I molecules depends on the MHC-peptide complex stability. *J. Immunol.* **156**, 3308–3314 (1996).
- Le Moullec, J. M. et al. The complete sequence of human preprocalcitonin. *FEBS Lett.* **167**, 93–97 (1984).
- Rusbridge, N. M. & Beynon, R. J. 3,4-Dichloroisocoumarin, a serine protease inhibitor, inactivates glycogen phosphorylase b. *FEBS Lett.* **268**, 133–136 (1990).
- Einstein, M. H. et al. Genetic variants in TAP are associated with high-grade cervical neoplasia. *Clin. Cancer Res.* **15**, 1019–1023 (2009).
- Leibowitz, M. S., Andrade Filho, P. A., Ferrone, S. & Ferris, R. L. Deficiency of activated STAT1 in head and neck cancer cells mediates TAP1-dependent escape from cytotoxic T lymphocytes. *Cancer Immunol. Immunother.* **60**, 525–535 (2011).
- Abele, R. & Tampe, R. Modulation of the antigen transport machinery TAP by friends and enemies. *FEBS Lett.* **580**, 1156–1163 (2006).
- Marincola, F. M., Jaffee, E. M., Hicklin, D. J. & Ferrone, S. Escape of human solid tumors from T-cell recognition: molecular mechanisms and functional significance. *Adv. Immunol.* **74**, 181–273 (2000).
- Setiadi, A. F. et al. Epigenetic control of the immune escape mechanisms in malignant carcinomas. *Mol. Cell. Biol.* **27**, 7886–7894 (2007).
- Lampen, M. H. et al. CD8⁺ T cell responses against TAP-inhibited cells are readily detected in the human population. *J. Immunol.* **185**, 6508–6517 (2010).
- Oliveira, C. C. et al. The nonpolymorphic MHC Qa-1b mediates CD8⁺ T cell surveillance of antigen-processing defects. *J. Exp. Med.* **207**, 207–221 (2010).
- van Hall, T. et al. Selective cytotoxic T-lymphocyte targeting of tumor immune escape variants. *Nat. Med.* **12**, 417–424 (2006).
- Wolfel, C. et al. Transporter (TAP)- and proteasome-independent presentation of a melanoma-associated tyrosinase epitope. *Int. J. Cancer* **88**, 432–438 (2000).
- Oliveira, C. C. et al. New role of signal peptide peptidase to liberate C-terminal peptides for MHC class I presentation. *J. Immunol.* **191**, 4020–4028 (2013).
- Martoglio, B. & Dobberstein, B. Signal sequences: more than just greasy peptides. *Trends Cell Biol.* **8**, 410–415 (1998).
- Borrego, F., Ulbrecht, M., Weiss, E. H., Coligan, J. E. & Brooks, A. G. Recognition of human histocompatibility leukocyte antigen (HLA)-E

- complexed with HLA class I signal sequence-derived peptides by CD94/NKG2 confers protection from natural killer cell-mediated lysis. *J. Exp. Med.* **187**, 813–818 (1998).
41. Pugsley, A. P. The complete general secretory pathway in gram-negative bacteria. *Microbiol. Rev.* **57**, 50–108 (1993).
 42. Martoglio, B., Graf, R. & Dobberstein, B. Signal peptide fragments of preprolactin and HIV-1 p-gp160 interact with calmodulin. *EMBO J.* **16**, 6636–6645 (1997).
 43. Henderson, R. A. et al. HLA-A2.1-associated peptides from a mutant cell line: a second pathway of antigen presentation. *Science* **255**, 1264–1266 (1992).
 44. Braud, V. M. et al. HLA-E binds to natural killer cell receptors CD94/NKG2A, B and C. *Nature* **391**, 795–799 (1998).
 45. Bland, F. A., Lemberg, M. K., McMichael, A. J., Martoglio, B. & Braud, V. M. Requirement of the proteasome for the trimming of signal peptide-derived epitopes presented by the nonclassical major histocompatibility complex class I molecule HLA-E. *J. Biol. Chem.* **278**, 33747–33752 (2003).
 46. El Hage, F., Durgeau, A. & Mami-Chouaib, F. TAP expression level in tumor cells defines the nature and processing of MHC class I peptides for recognition by tumor-specific cytotoxic T lymphocytes. *Ann. NY Acad. Sci.* **1283**, 75–80 (2012).
 47. Kincaid, M. M. & Cooper, A. A. Misfolded proteins traffic from the endoplasmic reticulum (ER) due to ER export signals. *Mol. Biol. Cell* **18**, 455–463 (2007).
 48. Vembar, S. S. & Brodsky, J. L. One step at a time: endoplasmic reticulum-associated degradation. *Nat. Rev. Mol. Cell Biol.* **9**, 944–957 (2008).
 49. Aletrari, M. O. et al. Eeyarestatin 1 interferes with both retrograde and anterograde intracellular trafficking pathways. *PLoS ONE* **6**, e22713 (2011).
 50. Coulie, P. G., Van den Eynde, B. J., van der Bruggen, P. & Boon, T. Tumour antigens recognized by T lymphocytes: at the core of cancer immunotherapy. *Nat. Rev.* **14**, 135–146 (2014).
 51. Chang, C. C. et al. Multiple structural and epigenetic defects in the human leukocyte antigen class I antigen presentation pathway in a recurrent metastatic melanoma following immunotherapy. *J. Biol. Chem.* **290**, 26562–26575 (2015).
 52. Chen, H. L. et al. A functionally defective allele of TAP1 results in loss of MHC class I antigen presentation in a human lung cancer. *Nat. Genet.* **13**, 210–213 (1996).
 53. Seliger, B. et al. Immune escape of melanoma: first evidence of structural alterations in two distinct components of the MHC class I antigen processing pathway. *Cancer Res.* **61**, 8647–8650 (2001).
 54. Kloor, M. et al. Immunoselective pressure and human leukocyte antigen class I antigen machinery defects in microsatellite unstable colorectal cancers. *Cancer Res.* **65**, 6418–6424 (2005).
 55. Mauerer, M. J. et al. Tumor escape from immune recognition: loss of HLA-A2 melanoma cell surface expression is associated with a complex rearrangement of the short arm of chromosome 6. *Clin. Cancer Res.* **2**, 641–652 (1996).
 56. Miyagi, T. et al. Impaired expression of proteasome subunits and human leukocyte antigens class I in human colon cancer cells. *J. Gastroenterol. Hepatol.* **18**, 32–40 (2003).
 57. Meissner, M. et al. Defects in the human leukocyte antigen class I antigen processing machinery in head and neck squamous cell carcinoma: association with clinical outcome. *Clin. Cancer Res.* **11**, 2552–2560 (2005).
 58. Lacroix, L. et al. Na(+)/I(-) symporter and Pendred syndrome gene and protein expressions in human extra-thyroidal tissues. *Eur. J. Endocrinol.* **144**, 297–302 (2001).
 59. Djenidi, F. et al. CD8+ CD103+ Tumor-infiltrating lymphocytes are tumor-specific tissue-resident memory T cells and a prognostic factor for survival in lung cancer patients. *J. Immunol.* **194**, 3475–3486 (2015).
 60. Wang, X. et al. A method to generate antigen-specific mAb capable of staining formalin-fixed, paraffin-embedded tissue sections. *J. Immunol. Methods* **299**, 139–151 (2005).
 61. Yang, Z. et al. Identification of new HLA-A*0201-restricted cytotoxic T lymphocyte epitopes from neuritin. *J. Neurooncol.* **114**, 51–58 (2013).
 62. Valmori, D. et al. Enhanced generation of specific tumor-reactive CTL in vitro by selected Melan-A/MART-1 immunodominant peptide analogues. *J. Immunol.* **160**, 1750–1758 (1998).
 63. Echchakir, H. et al. Evidence for in situ expansion of diverse antitumor-specific cytotoxic T lymphocyte clones in a human large cell carcinoma of the lung. *Int. Immunol.* **12**, 537–546 (2000).
 64. Echchakir, H. et al. Cytotoxic T lymphocytes directed against a tumor-specific mutated antigen display similar HLA tetramer binding but distinct functional avidity and tissue distribution. *Proc. Natl Acad. Sci. USA* **99**, 9358–9363 (2002).
 65. Dudley, M. E., Nishimura, M. I., Holt, A. K. & Rosenberg, S. A. Antitumor immunization with a minimal peptide epitope (G9-209-2M) leads to a functionally heterogeneous CTL response. *J. Immunother.* **22**, 288–298 (1999).
 66. Le Floch, A. et al. Alpha E beta 7 integrin interaction with E-cadherin promotes antitumor CTL activity by triggering lytic granule polarization and exocytosis. *J. Exp. Med.* **204**, 559–570 (2007).
 67. Wang, Q., Li, L. & Ye, Y. Inhibition of p97-dependent protein degradation by Eeyarestatin I. *J. Biol. Chem.* **283**, 7445–7454 (2008).
 68. Wang, Q. et al. The ERAD inhibitor Eeyarestatin I is a bifunctional compound with a membrane-binding domain and a p97/VCP inhibitory group. *PLoS ONE* **5**, e15479 (2010).
 69. Hermans, I. F. et al. The VITAL assay: a versatile fluorometric technique for assessing CTL- and NKT-mediated cytotoxicity against multiple targets in vitro and in vivo. *J. Immunol. Methods* **285**, 25–40 (2004).
 70. Perret, R. et al. Adjuvants that improve the ratio of antigen-specific effector to regulatory T cells enhance tumor immunity. *Cancer Res.* **73**, 6597–6608 (2013).
 71. Aspod, C. et al. A novel cancer vaccine strategy based on HLA-A*0201 matched allogeneic plasmacytoid dendritic cells. *PLoS ONE* **5**, e10458 (2010).
 72. Sanmamed, M. F. et al. Nivolumab and urelumab enhance antitumor activity of human T lymphocytes engrafted in Rag2-/-IL2Rgammanull immunodeficient mice. *Cancer Res.* **75**, 3466–3478 (2015).
 73. Franciszkievicz, K. et al. Intratumoral induction of CD103 triggers tumor-specific CTL function and CCR5-dependent T-cell retention. *Cancer Res.* **69**, 6249–6255 (2009).

Acknowledgements

We thank the cytometry facility (Plateforme d'Imagerie-Cytométrie) and the animal facility (Plateforme d'Evaluation Préclinique, PFEP) of Gustave Roussy. We also thank Olivia Bawa for help with IHC staining and Ludovic Lacroix for healthy thyroid tissue RNA. D122-HHD tumour cells were a generous gift from Lea Eisenbach, Weizmann Institute of Science, Israel. This work was supported by grants from the Association pour la Recherche sur le Cancer (ARC), Institut National du Cancer (INCa), Direction Générale de l'Offre de Soins (DGOS), Bpifrance and the Ligue contre le Cancer. S.C. is a recipient of the fund program "Equipe Labellisée Ligue 2015". A.D. was a recipient of a fellowship from INCa and Bpifrance. Y.V. was a recipient of a fellowship from INCa and the Université Paris-Sud.

Author contributions

Conception and design: A.D., F.M.-C.; development of methodology: A.D., Y.V., G.G., E. V., S.C., J.A., F.M.-C.; acquisition of data (providing animals, acquiring and managing patients, providing facilities, etc.): B.B., N.C., J.-C.S., Y.V., G.G., V.d.M., P.V., E.T., F.L., F. M.-C.; analysis and interpretation of data (e.g., statistical analysis, biostatistics, computational analysis): A.D., J.A., F.M.-C.; writing, review and/or revision of the manuscript: A.D., F.M.-C.; administrative, technical and material support (i.e., reporting and organizing data, constructing databases): A.D., G.G., F.D., Y.V., B.B., N.C., J.-C.S., V.d.M., P. V., S.C., A.E., S.F., F.M.-C.; study supervision: F.M.-C.

Additional information

Supplementary Information accompanies this paper at <https://doi.org/10.1038/s41467-018-07603-1>.

Competing interests: F.M.-C. is founder and consultant for ElyssaMed; A.D. is employee at ElyssaMed. The rest of the authors declare no competing interests.

Reprints and permission information is available online at <http://npj.nature.com/reprintsandpermissions/>

Publisher's note: Springer Nature remains neutral with regard to jurisdictional claims in published maps and institutional affiliations.



Open Access This article is licensed under a Creative Commons Attribution 4.0 International License, which permits use, sharing, adaptation, distribution and reproduction in any medium or format, as long as you give appropriate credit to the original author(s) and the source, provide a link to the Creative Commons license, and indicate if changes were made. The images or other third party material in this article are included in the article's Creative Commons license, unless indicated otherwise in a credit line to the material. If material is not included in the article's Creative Commons license and your intended use is not permitted by statutory regulation or exceeds the permitted use, you will need to obtain permission directly from the copyright holder. To view a copy of this license, visit <http://creativecommons.org/licenses/by/4.0/>.

© The Author(s) 2018